Mathematical Modelling of Vapor Explosions

N.S. Khabeev,[1] A.F. Bertelsen,[2] O.R. Ganiev[3]

Abstract

Vapor explosions, also called thermal detonation, occur when liquified gas comes into contact with water. During the contact of the two liquids with considerably different temperatures, intensive boiling of one of them takes place which is accompanied by an explosive increase in pressure. Similar phenomenon also arises in the cooling systems of nuclear power stations when as a result of some accident the heated particles of nuclear fuel settle in the cold water. This leads to the explosive boiling of the liquid and to a rapid increase of the pressure.

As a first stage this preprint presents analytical and numerical modelling of small scale single drops of liquified gas in water, and propagation of shock waves in liquids with bubbles containing evaporating drops of liquified gas.

Keywords: explosive boiling, liquified gas, vapor explosion, shock waves.

1 Introduction

Plans to exploit oil and gas fields in the Norwegian continental shelf usually include options to transport LNG (liquified natural gas) by ships to markets in Europe and America. The possibility of sinking, ship-ship collision or grounding needs to be considered in the development plans. Such accidents can of course occur near towns and other densely populated areas.

If LNG ship is involved in an accident such that large quantities of liquified gas escapes, a large explosion can occur (Bankoff 1978).

LNG ships are designed and operated to very high standards, because of the dangers involved in handling LNG. Nuclear power stations, similarly, are designed and operated to very high standard. Nevertheless, accidents do occur in nuclear power stations (Cronenberg 1980). It does not take much imagination to visualise an accident along the populated coast involving a LNG ship. The potential consequences of such an accident need to be known.

At this preprint small scale single drop explosions were modelled analytically and numerically and evolution of shock waves in liquids with bubbles containing evaporating drops of liquified gas was studied numerically.

[1]Dept. of Mathematics, University ov Bahrain, P.O.Box 32038, Bahrain
[2]Dept. of Mathematics, University of Oslo, P.O.Box 1053 Blindern, N–0316 Oslo, Norway
[3]Institute of Mechanics, Moscow University, P.O.Box 119899 Moscow, Russia

2 Dynamics of bubble containing evaporating liquid droplet

2.1 Formulation of the problem

The dynamics of gas and vapor bubbles was studied in many papers, discussed in reviews (Plesset & Prosperetti 1977, Feng & Leal 1997). Let us consider the behaviour of a spherical drop of liquified gas, surrounded by spherical vapor layer in the liquid. The processes occuring within the drop, bubble and around the bubble in the surrounding liquid are assumed to be spherically symmetric, so all parameters depend on time t and radial Eulerian coordinate r only. We assume that the "cold" drop and surrounding "hot" liquid are incompressible and ideal, and vapor can be described by the equation of state for perfect gas.

We will suppose also pressure uniformity within the bubble, which prevails when the size of the bubble is much less than the length of a sound wave in the gas (Nigmatulin et al 1981).

Within the framework of the assumptions made, the continuity, heat and state equations for gas phase will have the form (Nigmatulin et al 1981)

$$\frac{\partial \rho_g}{\partial t} + \frac{1}{r^2}\frac{\partial(\rho_g W_g r^2)}{\partial r} = 0$$

$$\rho_g C_g\Big(\frac{\partial T_g}{\partial t} + W_g\frac{\partial T_g}{\partial r}\Big) = \frac{1}{r^2}\frac{\partial}{\partial r}\Big(\lambda_g r^2\frac{\partial P_g}{\partial r}\Big) + \frac{dP_g}{dt} \tag{1}$$

$$P_g = \rho_g R_g T_g\,, \qquad b(t) \le r \le a(t)$$

where C_g, λ_g, R_g, W_g are specific heat of gas at constant pressure, thermal conductivity, gas constant, and velocity of the gas; $b(t)$ is the drop radius, $a(t)$ is the radius of the bubble. Here the subscripts d, g and ℓ refer to the parameters of the drop, gas, and surrounding liquid respectively.

The same equations for the liquid drop and surrounding liquid will have the form (Nigmatulin 1990)

$$\rho_d C_d\frac{\partial T_d}{\partial t} = \frac{1}{r^2}\frac{\partial}{\partial r}\Big(\lambda_d r^2\frac{\partial T_d}{\partial r}\Big)$$

$$W_d = 0\,, \qquad \rho_d = \text{const}\,, \qquad 0 \le r \le b(t) \tag{2}$$

$$\rho_\ell C_\ell\Big(\frac{\partial T_\ell}{\partial t} + W_\ell\frac{\partial T_\ell}{\partial r}\Big) = \frac{1}{r^2}\frac{\partial}{\partial r}\Big(\lambda_\ell r^2\frac{\partial T_\ell}{\partial r}\Big)$$

$$W_\ell r^2 = W_{\ell a}\, a^2\,, \qquad \rho_\ell = \text{const}\,, \qquad a(t) \le r$$

here $W_{\ell a}$ is the velocity of the liquid at the bubble surface ($W_{\ell a} = W_\ell(a)$).

The boundary conditions for equations (1), (2) at the centre of the drop, on the moving boundaries $b(t)$ and $a(t)$ and at infinity are (Nigmatulin 1990)

$$r = 0\colon \frac{\partial T_d}{\partial r} = 0$$

$$
\begin{aligned}
r = b(t)\colon & \begin{cases} \xi = \rho_g(W_{gb} - \dot{b}(t)) = -\rho_d \dot{b}(t) \\ T_{gb} = T_{db} = T_{sg}(P_g) \\ \lambda_g \frac{\partial T_g}{\partial r} - \lambda_d \frac{\partial T_d}{\partial r} = \xi \ell \end{cases} \\
r = a(t)\colon & \begin{cases} \lambda_g \frac{\partial T_g}{\partial r} = \lambda_\ell \frac{\partial T_\ell}{\partial r} \\ T_{ga} = T_{\ell a} \\ W_{ga} = \dot{a} = W_{\ell a} \\ P_{\ell a} = P_g - 2\sigma/a \end{cases} \\
r \to \infty \qquad & T_\ell \to T_\infty = \text{const} \qquad P \to P_\infty = \text{const}
\end{aligned} \tag{3}
$$

Here ℓ is the latent heat of evaporation of the drop, ξ is the of phase transition rate per unit interfacial surface ($\xi > 0$ for evaporation). $T_{sg}(P)$ is the saturation temperature; σ is the surface tension.

Being in the saturated state at the interface vapor obeys the Clapeyron-Clausius equation

$$
\frac{dT_{sg}}{dP_g} = \frac{T_{sg}}{\ell \rho_{gs}} \left(1 - \frac{\rho_{gs}}{\rho_d}\right) \tag{4}
$$

The Rayleigh equation for bubble oscillations in incompressible fluid has a form:

$$
a \frac{dW_{\ell a}}{dt} + \tfrac{3}{2} W_{\ell a}^2 = \frac{P_g - P_\infty - 2\sigma/a}{\rho_\ell} \tag{5}
$$

When the pressure uniformity condition in gas is satisfied, there is an integral of heat equation for the gas which can be obtained by substitution of continuity equation to heat equation and using equation of state (Nigmatulin 1990)

$$
\begin{aligned}
& \frac{dP_g}{dt} = \frac{3\gamma}{a^3 - b^3} \left(\lambda_g(T) r^2 \frac{\partial T_g}{\partial r}\right)\Big|_b^a - \frac{3\gamma P_g}{a^3 - b^3} (r^2 W_g)\Big|_b^a , \\
& f(r)\Big|_b^a = f(a) - f(b)
\end{aligned} \tag{6}
$$

The continuity equation for the gas with the use of the pressure uniformity condition and the boundary conditions, yields the velocity profile in the gas:

$$
W_g = \frac{b^2}{r^2} W_{gb} + \frac{1}{r^2 P_g} \left[\lambda_g(T) r^2 \frac{\partial T_g}{\partial r}\right]\Big|_b^r - \frac{r^3 - b^3}{3\gamma P_g r^2} \frac{dP_g}{dt} \tag{7}
$$

So, the system of basic equations consists now on three nonlinear equations of convectional heat conductivity in different space regions (in the drop, gas, and liquid), four ordinary differential equations (Rayleigh equation (5), Clapeyron-Clausius equation (4), equation for pressure (6), and equation for radius of the drop (3), and boundary conditions (3).

The considered problem is characterized by considerable variations of the vapor thermophysical parameters along the vapor layer. For example for the system sea water

(300K) – liquified hydrogen ($T_s = 22$K for $P =$ latm) or sea water (300K) and liquified helium ($T_s = 4.2$K for $p = 1$ atm) the thermal diffusivity coefficient $D_g = \lambda_g/\rho_g c_g$ is changing by a factor of fourty.

The high temperature gradient in the thin vapor layer ($T_\ell/T_s \gg 1$) leads to the strong variation of vapor density ($\rho_g = P_g/R_g T_g$) and thermal conductivity along the vapor layer. That is why it is very important to take into account the dependence of thermal conductivity on temperature in the heat equation for gas phase. Another thermophysical parameters: λ_d, ρ_d, C_d, C_g, ℓ, λ_ℓ, ρ_ℓ, C_ℓ can be considered as constants.

2.2 Discussion of the results

The problem was solved numerically using a finite-difference technique by dividing the whole system into spherical layers inside the drop and bubble and outside the bubble. There are two moving boundaries $b(t)$ and $a(t)$ at this problem. We used the new variables for "freezing" the moving boundaries:

$$
\begin{aligned}
&r \in (0, b(t)): \eta = \tfrac{r}{b(t)}\,, \qquad \eta \in (0,1) \\
&r \in (b(t), \infty): \xi = \tfrac{r-b}{a-b}\,, \qquad \xi \in (0,\infty)
\end{aligned}
\tag{8}
$$

So the boundaries now are not miving and fixed in the points

$$
\begin{aligned}
&r = 0 \leftrightarrow \eta = 0\,; \qquad r = b(t) \leftrightarrow \eta = 1, \qquad \xi = 0 \\
&r = a(t) \leftrightarrow \xi = 1\,; \qquad r \to \infty \leftrightarrow \xi \to \infty
\end{aligned}
\tag{9}
$$

With allowance made for the finite thermal conductivity of liquid, the boundary condition at infinity can be applied to the last layer of the liquid.

Calculations were made for different size $0.1-1.0$ mm of drops. Surrounding liquid was water at 293K. The initial pressure in the system was 1 atmosphere. We used different liquified gases at the saturation temperature. Thermophysical parameters were taken from (Vargaftik 1972).

Calculations made for different initial temperature distributions in the vapor indicate that initial temperature distribution has effect only on initial time interval. That is why we used as initial condition linear temperature distribution in the vapor.

Calculations show that the variation of the saturation temperature at the drop surface and variation of the interface bubble surface temperature are very small:

$$
\frac{T_s(P) - T_s(P_0)}{T_s(P_0)} \ll 1\,, \qquad \frac{T_{\ell a} - T_{\ell a 0}}{T_{\ell a 0}} \ll 1
\tag{10}
$$

Here the subscript 0 refers to the parameters of the initial state. So, it is possible to consider these temperatures as constants, and surrounding liquid as a thermostat. Hence it is possible to simplify the problem: don't solve the heat equations inside the frop and surrounding liquid, but solve it in the gas only.

Analysis of the evaporation process show that because $\rho_g \ll \rho_d$ the characteristic time of the drop radius change due to evaporation is much greater than the characteristic time

of heat processes. That is why at the time intervals, comparable with the characteristic time of heat processes the drop radius can be considered as constant. This was confirmed by calculations.

We computed variants corresponding to different drop and bubble radii, liquid and drop temperatures. Figure 1 illustrates the behaviour of pressure inside the bubble, containing the drop of liquified hydrogen ($b_0 = 0.1$ mm). The curves 1–3 correspond to different initial bubble size: $\frac{a_0}{b_0} = 1.05; 1.1; 1.2$ ($t_* = b_0^2/D_g$).

The calculations have shown that there are two stages of the process. First or dynamic stage is characterized by intensive pressure oscillations in the gas during the time interval $\sim b_0^2/D_g$. At this stage the pressure in the bubble can be considerably greater than intitial atmosphereic pressure. The second or thermal stage is characterized by the monotonic growth of the vapor bubble; pressure in the vapor is settled and equal to the external pressure $P_g = P_\infty$; the temperature profile is approaching to the quasistationary temperature distribution. The initial value of the vapor layer thickness has significant effect on the process at the dynamic stage.

The calculations have shown that decrease of the initial vapor layer thickness leads to an increase of the pressure oscillations amplitude and the oscillations attenuation time. The decrease of the initial vapor layer size leads also to a sharp increase of the evaporation rate and the velocity of bubble surface $\dot{a}$. This is connected with the growth of temperature gradient in the vapor phase due to the decrease of vapor layer thickness. Figure 2 illustrates the characteristic temperature and velocity profiles inside the bubble at different moments of time. $b_0 = 1$ mm, $a_0 = 1.1.$ mm. Curves 1–5 correspond to the moments of time $t/t_* = 0.1; 0.2; 0.5; 1.0; 5.0$. The calculations have shown that at the first stage of the process there is slight change of the initial linear temperature distribution in the gas phase, but the strong change of the velocity field. At the second thermal stage of the process the velocity profiles approaches to the quasi-steady configurations.

3 Shock waves in liquids with bubbles containing evaporating drops of liquified gas

The basic results of studying of a single bubble in a liquid volume are also valid for bubble mixtures with a low dispersed-phase volume concentration. The specific properties of the bubbly liquids include: the existence of internal small scale flows, the high density and compressibility of the medium, the low distrurbance propagation velocity, and the constancy of the carrier-phase density. In dynamic processes, however, one of the most interesting properties of bubbly liquids is the manifestation of local deformation inertia when the bubble volume changes and the elasticity of the gas in the bubble.

3.1 Basic assumptions

A mixture of liquid and two-pahse bubbles containing evaporating liquid droplets can be considered in the framework of the mechanics of interacting and interpenetrating continua, the first phase being the carrier liquid and the second the bubbles, each of which contains a

cryogenic-liquid droplet and its vapor. Similar problem when the bubbles contains heated solid particles was considered by Khabeev (1997). Wave processes in a liquid with bubbles containing liquid droplets are considered here under the following basic assumptions:

(i) the distances over which the flow parameters (for example, oscillatory wavelengths) vary significantly are much larger than the distances between the bubbles, which are themselves much larger than the bubble diameters (i.e. the volume fraction of the vapor phase is small enough, $\alpha_2 \lesssim 0.1$);

(ii) the mixture is locally monodispersed, i.e. in each material volume all the bubbles are spherical and of the same radius;

(iii) viscosity and thermal conduction are important only in the processes of interphase interaction and, in particular, in bubble pulsations;

(iv) nucleation, fragmentation, interaction and coagulation of the bubbles are absent;

(v) the velocities of the macroscopic motion of the phases coincide.

The last assumption allows us to describe bubble volume changes, temperature distributions inside and around the bubbles, condensation and evaporation in terms of the spherically symmetrical model using the equations for bubble radial pulsations and radial thermal conduction of the liquid.

3.2 System of equations of a liquid with two-phase bubbles

We will consider the closed system of equations for investigating the wave process in this medium. For one-dimensional plane motion, we will write the equations in the Lagrange coordinates x ant t. The conservation equations for the masses of each phases and number density are (Nigmatulin, Khabeev & Zuong 1988):

$$\frac{\partial \rho_1}{\partial t} + \frac{\rho \rho_1}{\rho_0}\frac{\partial v}{\partial x} = 0\ ; \quad \rho_1 = \rho_1^0 \alpha_1\ , \quad \rho_1^0 = \text{const}\ , \quad \rho = \rho_1 + \rho_2$$

$$\frac{\partial \rho_2}{\partial t} + \frac{\rho \rho_2}{\rho_0}\frac{\partial v}{\partial x} = 0\ ; \quad \rho_2 = \rho_2^* \alpha_2\ , \quad \alpha_2 = 4/3\pi a^3 n\ , \quad \alpha_1 + \alpha_2 = 1$$

$$\rho_2^* = (M_g + 4/3\pi d^3 \rho_d^0)/V_b\ , \quad V_b = 4/3\pi a^3\ , \quad \rho_d^0 = \text{const}\ , \quad \rho_2^* V_b = \text{const}$$

$$\frac{\partial n}{\partial t} + \frac{\rho n}{\rho_0}\frac{\partial v}{\partial x} = 0\ , \tag{11}$$

Here α is the volume concentration, n is the number of bubbles per mixture unit volume, ρ is the density, M_g is the vapor mass in the bubble, ρ_d^0 is the drop density, ρ_2^* is the two-phase bubble mean density, v is the velocity, d is the drop radius. The subscripts 1 and 2 refer to the carrier liquid and bubble phase, respectively. The subscript 0 refers to

the unperturbed parameters. The superscript 0 denotes the true material density. The balance equation for the mixture momentum is:

$$\frac{\partial v}{\partial t} + \frac{1}{\rho_0}\frac{\partial p}{\partial x} = 0\,, \qquad p = \alpha_1 p_1 + \alpha_2(p_2 - 2\Sigma/a) \tag{12}$$

here Σ is the surface tension coefficient, p is the pressure.

The Rayleigh equation for the radial fluid motion around a bubble, which takes the radial fluid inertia into account has the form:

$$\begin{aligned} &(1-\phi_1)a\frac{\partial w_1}{\partial t} + \tfrac{3}{2}(1-\phi_2)w_1^2 + \frac{4\nu_1}{a}w_1 = \frac{p_2 - p_1 - 2\Sigma/a}{\rho_1^0} \\ &\frac{\partial a}{\partial t} = w_1 = w_2 = w \\ &\phi_1 = \tfrac{3}{2}\frac{(\alpha_2)^{1/3} - \alpha_2}{1-\alpha_2}\,, \qquad \phi_2 = \frac{(\alpha_2)^{1/3}(2+\alpha_2) - 3\alpha_2}{1-\alpha_2} \end{aligned} \tag{13}$$

Here ν is the kinematic viscosity of the liquid, w is the radial velocity, ϕ_1 and ϕ_2 are correction coefficients for taking into account the "nonsingleness" of the bubble. These corrections characterize the difference of the fictitious pressure at infinity from the average pressure in the liquid.

Transfer processes in a two-phase mixture are determined by the distributions of microparameters near inhomogeneities. For an analysis not to be too complicated, one has to make use of models that could considerably simplify the microprocess equations. A possible model is one that employs the concept of a cell with a test bubble in it at any point specified by a vector x. The cell dimensions are determined by the volume fractions of the phases and equal to $a\alpha_2^{1/3}$, the cell centre coinciding with the centre of the test bubble. This cell moves with the macroscopic velocity $v(t,x)$ of the vapour phase at the point considered. The distributions of microparameters inside a cell are described by the equations for the corresponding microprocesses with the boundary conditions on the test bubble surface (which determine the interphase interaction) and on the external boundary of the cell (which determine the action of the external, relative to the cell, carrying phase).

For describing the nonstationary interphase heat and mass transfer, we will use a spherically symmetric "trial" bubble model. We will consider a trial bubble with a cryogenic liquid droplet at its center. We assume that the temperature of the surrounding liquid (water) is much higher than cryogenic liquid boiling point. The liquid droplet evaporates and forms a vapor layer. The temperature of microparticles of droplet, vapor and surrounding liquid will depend on macrocoordinate x, radial microcoordinate r, counted from the test bubble center and time t

$$T_i' = T_i'(x,r,t) \qquad (i = 1, 2_d, 2_g)$$

For $T_i'(x,r,t)$ we have the heat equations inside the droplet ($r \le d$) in vapor ($d \le r \le a$), and in liquid ($r \ge a$). The radial velocity of the liquid w_1' is determined from the continuity

equation for incompressible liquid. The radial velocity of the vapor w'_{2g} can be determined from the continuity equation taking into account the equation of state

$$P'_2 = R_g T'_{2g} \rho'_{2g}$$

and homobaricity (pressure uniformity) in the vapor phase: $P'_2 = P_2(x,t)$.

In 2.2 was shown that the heat processes inside the droplet and in surrounding liquid are insignificant, and the temperature of the droplet can be considered as uniform and equal to the saturation temperature, and temperature of the surrounding liquid is constant:

$$T'_{2d} = T'_{2d}(x,t) = T_s(P_2)\ , \qquad T'_1 = \text{const}$$

According to Clapeyron-Clausius equation

$$\frac{\partial T_s}{\partial t} = \frac{T}{\ell \rho^0_{2s}}\Big(1 - \frac{\rho^0_{2s}}{\rho^0_{2d}}\Big)\frac{\partial P_2}{\partial t}\ , \qquad \rho^0_{2s} = \rho^0_{2g}{}'(T_s, P_2) \tag{14}$$

here ℓ is the latent heat of evaporation, the subscript s refers to the saturation parameters.

A numerical study of this system of equations would take too much CPU time. A simplification of the system is required. A numerical analysis indicates that the quasi-steady solution of the heat conduction equation in the vapor layer, which takes into account the temperature dependence of the vapor thermal conductivity, is a good approximation of the exact solution. For the time intervals under consideration, the droplet radius change can be neglected. Accordingly, we obtain the following relations for the pressure and mass of the vapor:

$$\begin{aligned}
&\frac{a^3 - d^3}{3(\gamma - 1)}\frac{\partial p_2}{\partial t} = \frac{ad}{a-d}KT'_1 - \frac{\gamma}{\gamma - 1}p_2 w'_1(x,a,t) \\
&\frac{\partial M_g}{\partial t} = 4\pi \frac{ad}{a-d}\frac{K}{c_g}\ , \qquad \lambda_g(T) = AT'_{2g} + B \\
&K = A(T'_1 - T_s) + (B - A(\ell/c_g - T_s))Ln\Big(1 + \frac{T'_1 - T_s}{\ell/c_g}\Big)
\end{aligned} \tag{15}$$

here γ is the specific heat ratio, c_g is the specific heat of vapor at constant pressure.

In the problem under consideration, the temperature dependence of the vapor thermal conductivity must be taken into account, the simplest approximation used in the literature being linear (Vargaftik 1972). The system of basic equations was transformed to a form suitable for numerical integration:

$$\begin{aligned}
&\frac{\partial \rho}{\partial t} = -3\frac{\alpha_2 \rho w}{a} \\
&\frac{\partial v}{\partial x} = 3\frac{\alpha_2 \rho_0 w}{\rho a} \\
&\frac{\partial^2 p}{\partial x^2} + F_x(x)\frac{\partial p}{\partial x} = G(p, p_2, \alpha_2, a, w) \\
&(1 - \phi_1)a\frac{\partial w}{\partial t} + \tfrac{3}{2}(1-\phi)w^2 + \frac{4\nu_1}{a}w = \frac{p_2 - p - 2\Sigma/a}{\alpha_1 \rho^0_1}
\end{aligned} \tag{16}$$

$$\frac{\partial a}{\partial t} = w$$
$$\frac{\partial T_s}{\partial t} = \frac{T_s}{\ell\rho^0_{2s}}\Big(1 - \frac{\rho^0_{2s}}{\rho^0_{2d}}\Big)\frac{\partial p_2}{\partial t}\ , \qquad \rho^0_{2s} = p_2/R_gT)$$
$$\frac{a^3 - d^3}{3(\gamma-1)}\frac{\partial p_2}{\partial t} = \frac{ad}{a-d}KT_1 - \frac{\gamma}{\gamma-1}p_2 w$$
$$\frac{\partial M_g}{\partial t} = 4\pi\frac{ad}{a-d}\frac{K}{c_g}\ ,$$

$$\rho = \rho_1 + \rho_2\ , \quad \rho_1 = \rho^0_1\alpha_1\ , \quad \rho^0_1 = \text{const}\ , \quad \rho_2 = \rho^*_2\alpha_2\ , \quad \alpha_1 = 4/3\pi a^3 n\ ,$$
$$\alpha_1 + \alpha_2 = 1\ , \quad \rho^*_2 = (M_g + 4/3\pi d^3\rho^0_d)/V_b\ , \quad V_b = 4/3\pi a^3\ , \quad \rho^0_d = \text{const}\ ,$$

$$\rho^*_2 V_b = \text{const}\ , \quad p = \alpha_1 p_1 + \alpha_2(p_2 - 2\Sigma/a)\ , \quad T_1 = \text{const}$$
$$\phi_1 = \frac{3}{2}\frac{(\alpha_2)^{1/3} - \alpha_2}{1-\alpha_2}\ , \qquad \phi_2 = \frac{(a_2)^{1/3}(2+\alpha_2) - 3\alpha_2}{1-\alpha_2}$$
$$K = A(T_1 - T_s) + (B - A(\ell/c_g - T_s))Ln\Big(1 + \frac{T_1 - T_s}{\ell/c_g}\Big)$$
$$(\lambda_g(T) = AT_{2g} + B)$$
$$F_x(x) = -\frac{1}{\rho_0}\frac{\partial\rho_0}{\partial x}\ ,$$
$$G = -\frac{3\alpha_2\rho_0^2}{(1-\phi_1)\rho a^2}\Big[\frac{w^2}{2}(1 - 4\phi_1 + 3\phi_2) - \frac{4\nu_1}{a}w + \frac{1}{\alpha_1\rho^0_1}(p_2 - p - 2\Sigma/a)\Big]$$

The system (16) is separated. The mixture density, saturation temperature, pressure in the bubble, bubble radius and radial velocity are determined from differential equations which don't contain the derivatives relative to x. The average pressure and mixture density are determined from linear differential equations which don't contain the derivatives relative to t. These two equations allow us to determine the velocity and pressure fields of the mixture at fixed instants through the known fields of the remaining parameters.

The initial conditions correspond to the uniform state:

$$t = 0\ , \quad P_1 = p_0\ , \quad p_2 = p_0 + 2\Sigma/a_0\ , \quad a = a_0\ , \quad T_s = T_s(p_0)\ ,$$
$$\alpha_2 = \alpha_{20}\ , \quad w = v = 0\ , \quad M_g = M_{g0} \tag{17}$$

where initial mass of the vapor M_{g0} is determined by integrating the vapor density over the vapor layer thickness using initial temperature profile. At $x = 0$ and $x = L$, the boundary conditions have the form

$$x = 0\text{:} \quad P = f(t) \tag{18}$$
$$x = L\text{:} \quad \frac{\partial P}{\partial x} = 0 \qquad \text{or} \quad P = P_0\ . \tag{19}$$

In the case of shock waves: $f(t) = p_1 = \text{const}$. The relation between Eulerian and Langrangian coordinates is:

$$y(x,t) = \int_0^t V(x,\tau)d\tau \tag{20}$$

The system of basic equations with corresponding initial and boundary conditions can be used for studying the general regularities of propagation of plane nonstationary waves. The solution of this multiparameter problem depends on the nondimensional combinations characterizing the role of capillary effects, the liquid viscosity in radial bubble oscillations, the volume fraction, the sizes of the droplet and bubble, the thermophysical properties of the liquid and vapor, and the shock wave strength. In addition, the process depends on the shape of the initial impulse, its duration, and the initial conditions.

3.3 Numerical study of wave processes in a liquid with two-phase bubbles

Equations (16) with initial and boundary conditions were solved numerically using a combination of the sweep method for the partial differential equation (for determining the mixture pressure field) and the Euler method for ordinary differential equations.

For checking and debugging the computer program, we calculated the evolution of compression waves in vapor-liquid mixtures without liquid droplets. The numerical results are in a good agreement with the data of (Nigmatulin, Khabeev & Zuong 1988).

The evolution of shock-waves was investigated for the mixture of water with liquid hydrogen droplets surrounded by vapor shells. The following values of the thermophysical parameters were used:

$$\begin{aligned}
&p_0 = 1 \text{ bar}\,, \quad \Delta p = 0.2 \text{ bar}\,, \quad T_0 = 300\,\text{K}\,, T_{s^0} = 22\,\text{K}\,,\\
&\rho_1^0 = 963 \text{ kg/m}^3\,, \quad \rho_{g^0}^0 = 0.08 \text{ kg/m}^3\,, \quad \rho_d^0 = 70.92 \text{ kg/m}^3\,,\\
&c_g = 1.15 \cdot 10^4 \text{ J/(kg} \cdot \text{K)}\,, \quad \ell = 4.6 \cdot 10^5 \text{ J/kg}\,.\\
&\lambda(T_0) = 1.83 \cdot 10^{-1} \text{ W/(m} \cdot \text{K)}\,, \quad \lambda(80\,\text{K}) = 5.32 \cdot 10^{-2} \text{ W/(m} \cdot \text{K)}
\end{aligned}$$

Figures 3 and 4 show the profiles of the mixture pressure at different instants of time before and after wave reflection from the rigid wall. Due to local deformation inertia, as a result of the conversion of the kinetic energy input of the wave into potential compression energy, the mixture pressure $p(x,t)$ may be greater than the amplitude of the original wave.

The wave propagates in a mixture with increasing pressure rather than in one with uniform parameters. This is because, as distinct from mixtures with gas or vapor bubbles, the wave is preceded by a process of liquid droplets evaporation into the vapor layer and hence a pressure increase in the vapor layer and in the mixture. The oscillations in the reflected wave (Fig. 4) have nonlinear character and their maximum amplitude is considerably higher than the amplitude of the original wave.

To study the effect of initial pressure on the process, we computed a variants for a mixture at high initial static pressure. In this case, due to the increased liquid boiling

point and increased wave velocity the nonstationarity of the state ahead of the shock wave had almost no effect.

When the other conditions are fixed, an increase in the initial pressure results in a decrease in the interphase heat and mass transfer rates and, hence, in an increase in the pulsations during shock wave propagation. Clearly, as the initial static pressure in the system increases, the length of relaxation to the steady-state regime also increases. This is attributable to the increase in not only the wave velocity but also the vapor mass in the vapor layer for a fixed initial radius, since the vapor density increases. This leads to a marked increase of the role of the vapor inertia.

Figure 5 illustrates the profiles of the mixture pressure before and after reflection from rigid wall. The reflection has a nonlinear character. The reflection coefficient of shock wave in Figure 5

$$K_p > 4\,, \qquad K_p = \frac{P^1_{\max} - P^0_{\max}}{P^0_{\max} - P_0}\,,$$

where $P^0_{\max}$ is the maximum wave pressure before the reflection, and $P^1_{\max}$ is the maximum pressure at the wall surface during the reflection. So the shock strength at the rigid wall surface can be considerably greater than the amplitude of the incident wave.

Figure 6 shows the behaviour of the pressure at the wall surface during the time.

The maximum value of the pressure at the wall surface depends on the amplitude of the wave, and also on concentration of phases and bubble size (dispersity). Increasing of disperse phase concentration leads to the increasing of pressure amplitude on the wall surface.

Figure 7 shows the profiles of the mixture pressure at different instants of time for another boundary condition at the $x = L$: $p = p_0$. The *rarefaction* wave is propagating from the right side. First this wave is propagating in undisturbed area with increasing pressure, and later this wave makes shock wave weeker.

We computed variants corresponding to different bubble and droplet radius, volume concentrations, and initial pressure. Varying a droplet radius at some constant initial bubble radius affects the liquid evaporation rate and hence the rate of pressure increase ahead of the shock wave. An increase in droplet radius leads to more intense liquid evaporation, due to the decrease in vapor layer thickness, and to a wave velocity increase. With decrease in the ratio of the drop and initial bubble radii, a smooth passage to a liquid-vapor mixture with single-phase bubbles (without droplets) takes place.

It is shown that unlike to liquids with single-phase bubbles in liquids with two-phase bubbles decrease of the initial bubble size leads to increasing of the amplitude of oscillations. This is caused by the intensification of droplets evaporation due to the increasing of interfacial surface.

Conclusion

A mathematical model to describe the dynamics of bubble containing the dropelt of liquified gas with allowance for the nonlinear non-steady interphase heat and mass transfer has been proposed. General regularities of the behaviour of such "two-phase" bubble

depending on the initial conditions and thermophysical properties of phases have been studied on the basis of this model.

Wave evolution and reflection in a liquid with two-phase bubbles each containing a droplet of liquified gas is studied numerically. The influence of the basic governing parameters on the structure and evolution of waves in these media is investigated. The phenomenon of the nonlinear anomalous enhancement of waves reflected from a rigid wall is established.

The proposed models can be useful for analysis and understanding of such complicated phenomenon as vapor explosion.

Acknowledgements

This work was supported by the Norwegian Research Council (grant No 110560/410).

References

[1] Bankoff, S.G., 1978. Vapour Exposions: A Critical Review, in: Proc. of the 6th Int. Heat Transfer Conf. Toronto, Canada, V.6: 355–366, National Research Council of Canada, Toronto.

[2] Cronenberg, A.W., 1980. Recent Developments in the Understanding of Energetic Molten Fuel-Coolant Interactions. *Nuclear Safety*, **21** (3): 319–337.

[3] Feng, Z.C., and Leal, L.G., 1997. Nonlinear Bubble Dynamics. *Ann. Rev. Fluid Mech.* **29**, 201–243.

[4] Khabeev, N.S., 1997. Shock-wave Evolution in a Liquid with "Two-phase" Bubbles. *Fluid Dynamics*, **32** (2): 245–251.

[5] Nigmatulin, R.I., Khabeev, N.S., and Nagiev, F.B., 1981. Dynamics, Heat and Mass Transfer of Vapour-Gas Bubble in Liquid. *Int. J. Heat Mass Trans.* **24** (6): 1033–1044.

[6] Nigmatulin, R.I., Khabeev, N.S., and Zuong, N.H., 1988. Waves in Liquids with Vapour Bubbles. *J. Fluid Mech.* **186**, 85–117.

[7] Nigmatnlin, R.I., 1990. *Dynamics of Multiphase Media.* Washington, D.C.: Hemisphere.

[8] Plesset, M.S., and Prosperetti, A., 1977. Bubble Dynamics and Cavitation. *Ann. Rev. Fluid Mech.* **9**, 145–185.

[9] Vargaftik, N.B., 1972. *Handbook of Thermophysical Properties of Gases and Liquids.* (in Russian) Moscow: Nauka.

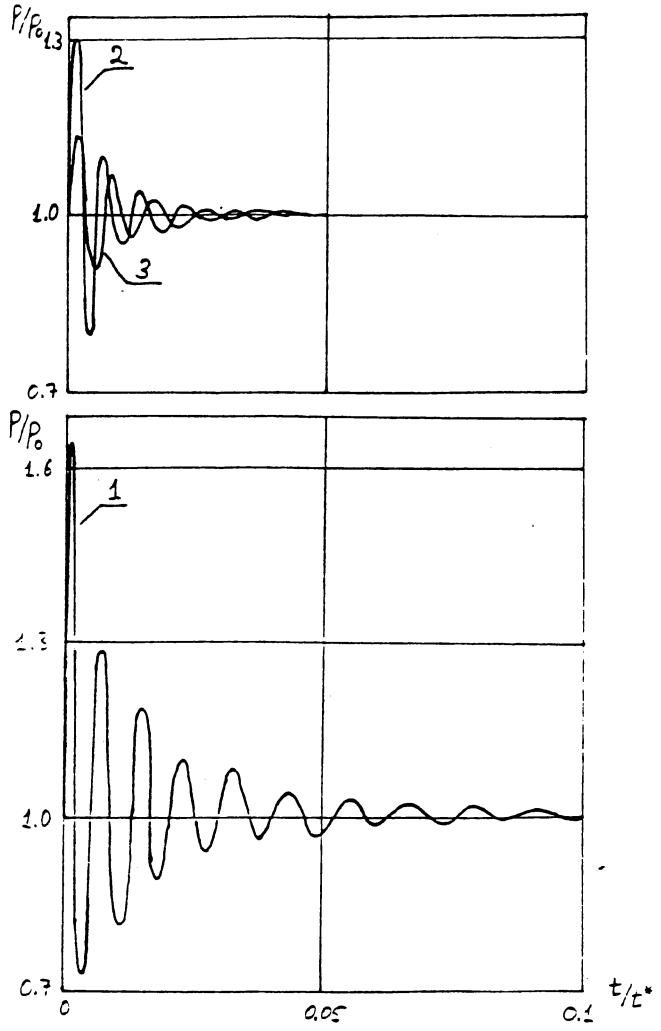

Figure 1: Pressure vs time curve for the bubble containing the droplet of liquified hydrogen ($b_0 = 0.1$ mm). The curves 1–3 correspond to different initial bubble size: $a_0/b_0 = 1.05$; 1.1; 1.2.

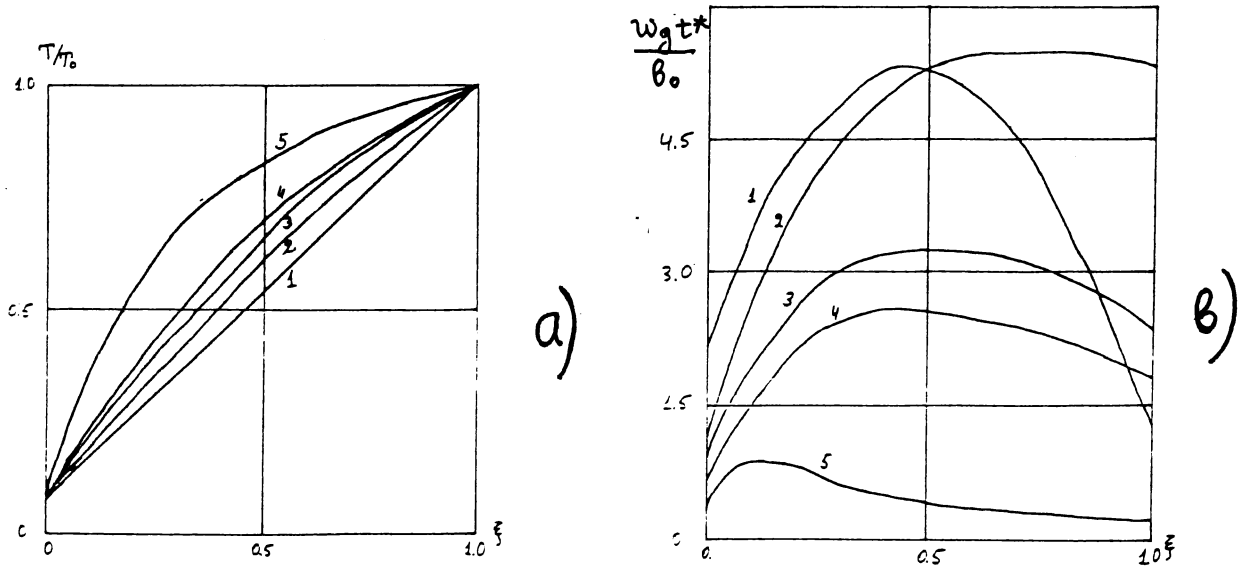

Figure 2: Evolution of the temperature (a) and velocity (b) profiles inside the vapor layer. $b_0 = 1$ mm, $a_0 = 1.1$ mm. Curves 1–5 correspond to the moments of time: $t/t_* = 0.1$; 0.2; 0.5; 1.0; 5.0.

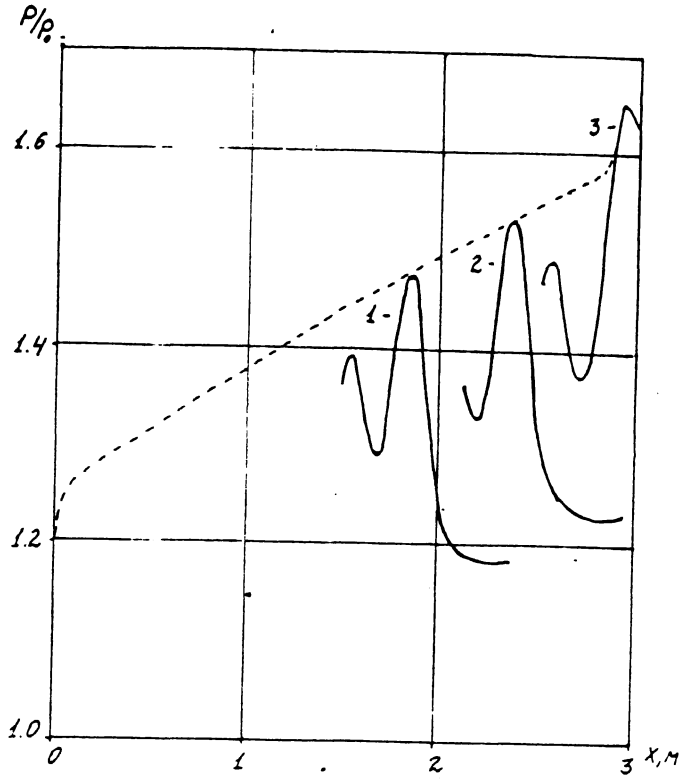

Figure 3: Pressure wave profiles before reflection from rigid wall. Curves 1–3 correspond to times: $t = 20$ ms; 25 ms; 30 ms. The dashed curve is the envelope of pressure peaks. $d = 1$ mm, $a_0 = 5$ mm, $\alpha_{20} = 0.02$, $P_\infty/P_0 = 1.2$.

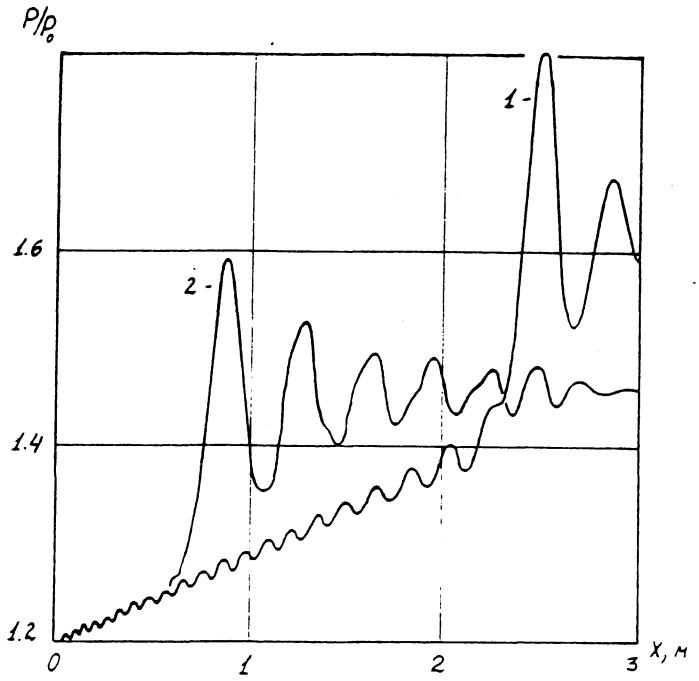

Figure 4: Pressure wave profiles after reflection from rigid wall. Curves 1, 2 correspond to times: 35 ms, 50 ms. Parameters are the same as in Figure 3.

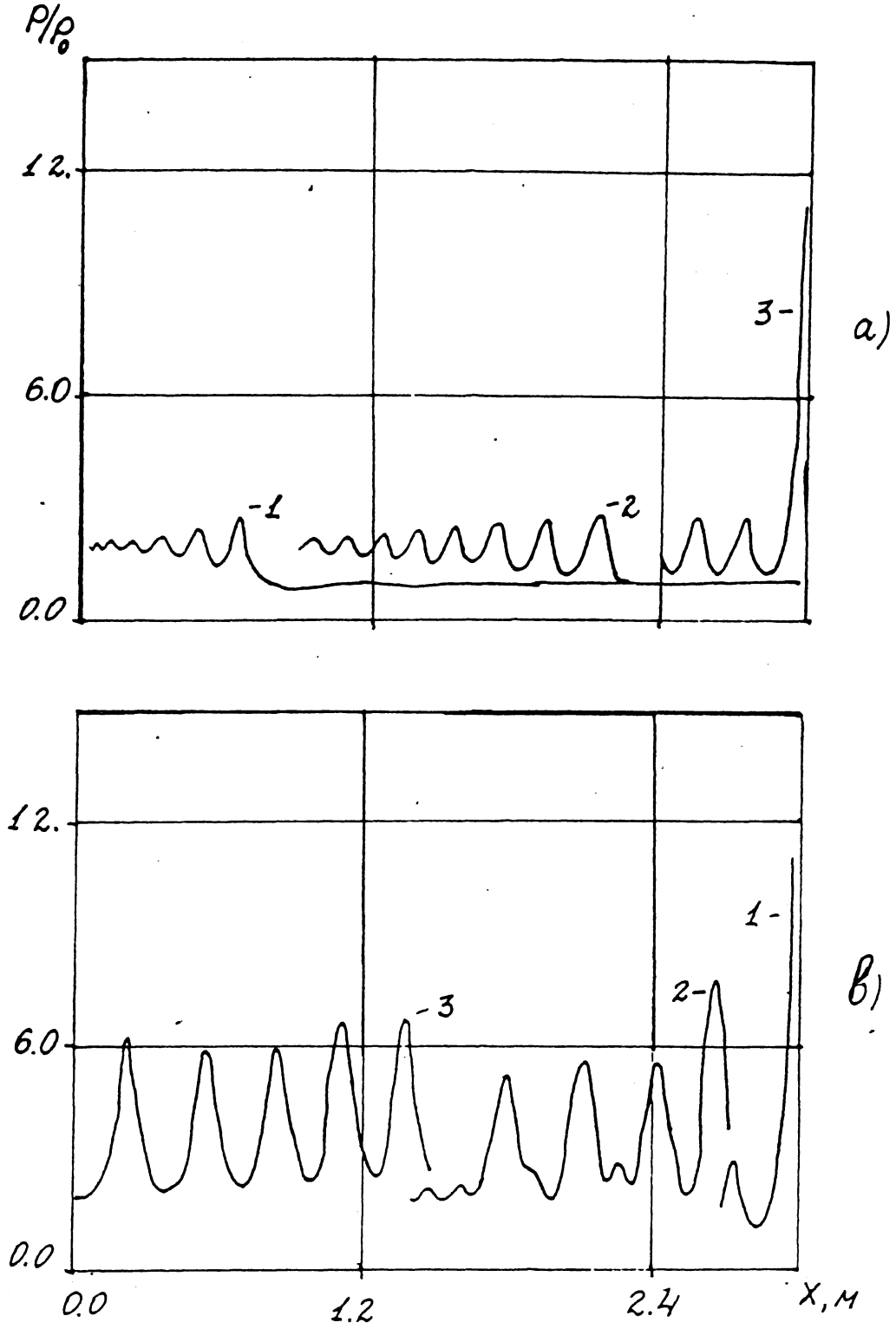

Figure 5: Pressure wave profiles before and after reflection from rigid wall. $d = 0.5$ mm; $a_0 = 2.5$ mm; $\alpha_{20} = 0.005$; $P_\infty/P_0 = 2$. Curves 1–3 correspond to times:
a) 1 ms; 3 ms; 4.125 ms
b) 4.125 ms; 5 ms; 6 ms.

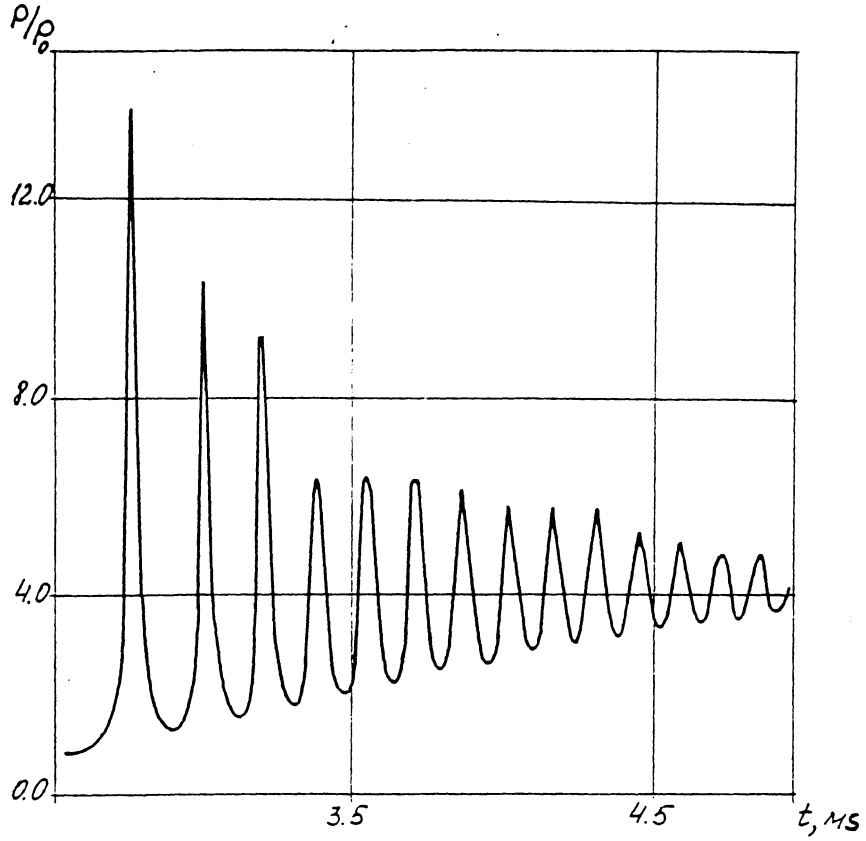

Figure 6: Pressure at the surface of rigid wall vs time. $\alpha_{20} = 0.005$; $d = 0.5$ mm; $a_0 = 2.5$ mm; $P_\infty/P_0 = 2$.

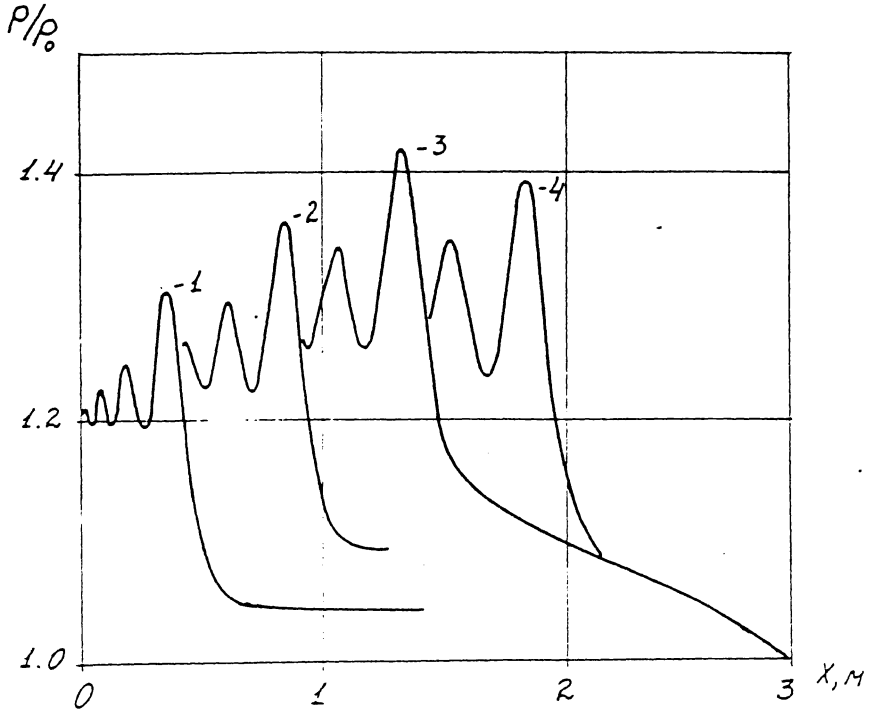

Figure 7: Pressure profiles at different moments of time. Curves 1–4 correspond to times: 5 ms; 10 ms; 15 ms; 20 ms. $d = 1$ mm; $a_0 = 5$ mm; $\alpha_{20} = 0.02$; $P_\infty/P_0 = 1.2$.